Journal of the European Ceramic Society 22 (2002) 903–916

www.elsevier.com/locate/jeurceramsoc

A study of slag-infiltrated magnesia-chromite refractories using hybrid microwave heating

P.T. Jones *, J. Vleugels, I. Volders, B. Blanpain, O. Van der Biest, P. Wollants

Department of Metallurgy and Materials Engineering (MTM), Katholieke Universiteit Leuven, W. De Croylaan 2, B-3001 Leuven, Belgium

Received 19 October 2000; accepted 27 November 2000

Abstract

Rebonded magnesia-chromite refractories are used in vacuum oxygen decarburisation ladles for the secondary refining of stainless steel. They suffer from acute wear due to the stringent chemical, thermal and mechanical conditions imposed. Although post-mortem investigation of worn refractories is indispensable to study the degradation mechanisms, its application is often hampered by evaluation difficulties due to crystallisation phenomena occurring during in situ cooling. To study the actual microstructures at elevated temperatures, industrially worn and virgin refractory samples were reheated and quenched in a cylindrical single-mode microwave furnace. Usage of a tubular susceptor allowed reproducible hybrid heating of the samples up to 1800°C. The quenched samples were analysed with SEM and EPMA-EDS. Concurrently, elemental line scans, X-ray mappings and quantitative image analyses were performed. This allowed the description of the 'high-temperature inactivation' mechanisms of the secondary chromite bonding phase: dissolution (1) in the periclase phase and (2) in the liquid slag, with (2) being predominant. Conclusions are drawn with respect to the refractoriness of the contributors to the spinel bonding phase: $MgO.Cr_2O_3$ (magnesiochromite) > $MgO.Al_2O_3$ (spinel)≫$MgO.Fe_2O_3$ (magnesioferrite). Hybrid microwave heating is shown to be an interesting alternative for conventional furnace experiments on refractory samples.

Keywords: Corrosion; Wear resistance; Spinel; Refractories; Magnesia-chromite; Microwave heating

1. Introduction

Direct-bonded or rebonded magnesia-chromite refractories are typically used in vacuum oxygen decarburisation (VOD) ladles for the secondary refining of stainless steels, due to their attractive mechanical and refractory properties such as high hot temperature strength, resistance to slag attack and dimensional stability. However, in the slag line of VOD ladles this refractory type suffers from acute wear as a result of the stringent thermal, mechanical and chemical stresses imposed. The dominant degradation mechanisms of magnesia-chromite refractories in VOD ladles have been intensively investigated in previous studies[1–5] by post-mortem analysis (mainly with SEM, EPMA-EDS and XPS) of bricks taken from different locations in the ladle. The combination of high processing temperatures (occasionally exceeding 1750°C), aggressive silicate slags and low pressures (0.1–20 kPa) has been shown to be detrimental, especially to the refractories contacting the slag phase. Three kinds of interrelated degradation phenomena occur: (1) infiltration of silicate slags into the refractory and chemical reaction with the refractory phases, leading to continuous erosion processes, (2) spalling and discontinuous wear due to abrupt temperature changes, and (3) decomposition of chromite and periclase phases as a result of the low oxygen partial pressure ($< 10^{-4}$ Pa).[1,3] Post-mortem analysis has been indispensable to unravel these highly interactive degradation mechanisms. However, when examining industrially worn samples, one is always restricted by the imperfect quenching of the lining (through exposure to the ambient air during continuous casting) as it is evident that one cannot simply take a refractory sample from a hot VOD ladle. The imperfect quenching of these refractories results in crystallisation and diffusion phenomena inside the brick, hindering the evaluation of the degradation mechanisms.

In this work, the latter problem was overcome by laboratory furnace heating/quenching experiments. To study the actual high temperature magnesia-chromite refractory microstructures, both industrially worn as

* Corresponding author.
E-mail address: peter.jones@mtm.kuleuven.ac.be (P.T. Jones).

0955-2219/02/$ - see front matter
PII: S0955-2219(00)00343-5

virgin refractories were slowly heated in a microwave furnace, held at a temperature of typically between 1300 and 1800°C, quenched, and analysed with SEM and EPMA.

In the literature a number of similar studies on the microstructure and properties of magnesia-chromite and chromite-magnesia refractories at high temperatures are available. Dewendra et al.[6] investigated the microstructure of a series of mixtures containing different proportions of commercial magnesia and chrome ore by quenching pressed specimens from temperatures in the range of 1400–1700°C and analysing them with EPMA. Hayhurst and Laming[7] studied the structure of chromite-magnesia refractories at high temperatures (from 1360 to 1700°C) by quenching the samples in air and assessing them with SEM. Both studies were performed in a molybdenum-wound laboratory furnace. Apart from these papers, a number of related studies can be found in the literature.[8–11]

The novelty of this study is four-fold. Firstly, instead of a conventional furnace a newly developed single-mode microwave furnace was used for the heating/quenching experiments. Secondly, temperatures up to 1800°C were achieved. Such temperatures are required to simulate the VOD process conditions, where temperatures in excess of 1700°C (i.e. the maximum in existing studies) are frequently obtained. Thirdly, not only the high-temperature behaviour of as-delivered refractories was investigated, but also industrially worn — heavily slag infiltrated — materials were assessed. Comparison of the relatively slowly in situ cooled industrial samples and the reheated/quenched counterparts leads to additional understanding of the refractory behaviour under harsh conditions. Finally, a detailed analysis of the distribution of the various elements present in the brick was performed using line scans and X-ray mapping experiments. The results were coupled with the existing knowledge on magnesia-chromite refractory degradation in VOD ladles. This study therefore allowed a more comprehensive understanding of the detrimental effect of the 'high-temperature inactivation' of the secondary chromite (direct) bonding phase in commercial magnesia-chromite refractories.

2. Experimental procedures

2.1. Hybrid microwave heating furnace

The microwave furnace used in this study was designed and manufactured by MEAC (Leuven, Belgium). The furnace consists of a 2.45 GHz microwave generator with a continuously adjustable power output from 0 to 2000 W, a cylindrical single-mode tuneable applicator, and an Eurotherm control system. Single-mode microwave systems result in a small, fully characterised, reproducible, inexpensive, user-friendly and easy to maintain microwave cavity. The drawback of single-mode cavities is their relatively small uniform electromagnetic field volume, which only allows uniform heating of relatively small specimens (see Fig. 1).

Microwave heating is a process in which a material couples with microwaves, volumetrically absorbs the electromagnetic energy, and transforms it into heat. The parameter that determines the coupling ability is the dielectric loss factor, according to which materials can be classified as transparent (low loss factor), opaque (conductor) or absorbing (high loss factor). The dielectric loss factor usually increases exponentially with temperature. Oxidic refractory materials typically show a low loss factor at room temperature, resulting in problematic coupling at low temperatures. The absence of 'room temperature coupling' is one of the major problems encountered in microwave-only heating. Tests with microwave-only heating were indeed unsuccessful, as a long warming up time

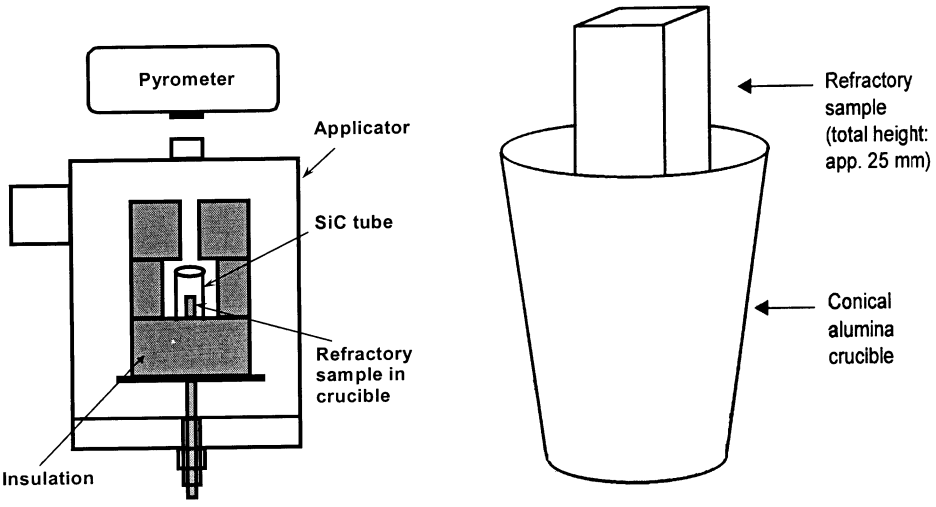

Fig. 1. Experimental setup in the MEAC single-mode microwave cavity (a) and a detailed illustration of the refractory sample/crucible setup (b).

was required before the refractory material started coupling with the microwaves. Furthermore, there is the risk of plasma formation in the cavity. To avoid these problems, hybrid heating (with a cylindrical SiC susceptor surrounding the sample contained in an alumina crucible) was used to establish immediate heating as well as smooth and reproducible temperature versus time curves. The SiC susceptor has a high loss factor and, therefore, couples well with microwaves, even at room temperature. Therefore, in the beginning of the heating cycle, the applied microwave energy is used to heat the susceptor, which conventionally heats the crucible and the sample. As the temperature of the crucible and sample reach a certain critical temperature, they also start coupling with the microwaves. In this way, hybrid heating, the combination of microwave and conventional heating, is achieved.

By comparison of the sintering process of $BaTiO_3$ (high loss factor) and ZrO_2 (low loss factor) ceramics, Zhao and Vleugels[12] unambiguously proved that the heating achieved with this setup is indeed of the hybrid type, as microwaves were shown to partially penetrate the thin susceptor causing volumetric heating in the samples.

Compared to conventional heating, hybrid heating clearly shows advantages with respect to warm-up time, energy consumption and quenching possibilities. Especially the latter can be of great significance when studying refractory structures at high temperatures.

Fig. 1 shows the experimental setup in the microwave cavity. A home-made cylindrical SiC tube, with a diameter of 19 mm, a height of 28 mm and a wall thickness of 2 mm, was used as susceptor.[12] The refractory specimen was placed in a conical alumina (99.7 wt.%) crucible. The latter was required to contain liquid slag-like phases which are formed at sufficiently high temperatures. A porous fibrous mullite refractory was used as insulation material. Temperature was controlled by a two-colour pyrometer (Type M90-R1, MIKRON) focused on the top face of the refractory sample. Since the temperature measurement range of this instrument is limited to 700–2000°C, the recording of the heating curves only starts from 700°C.

The maximum applied microwave power input was 350 W. The atmosphere was controlled by blowing nitrogen (Type N28) into the furnace with a flow rate of 600 l/h. The refractory specimens were slowly heated at 20°C per min to a predefined temperature, with a dwell time of 25 min to achieve full homogenisation and to simulate industrial refractory exposure time. The samples were subsequently quenched to room temperature. This process occurred in two stages. As soon as the microwave power supply was switched off, primary quenching rates of typically 300°C during the first 10 s were recorded. The furnace could then be instantaneously opened. After which, the insulation material, susceptor and refractory sample were removed and exposed to the ambient air for secondary quenching until room temperature.

The maximum obtained temperature with this experimental setup was 1800°C. At that temperature, the porous insulation material started coupling with the microwaves as well, causing thermal runaway and the formation of hot spots in the insulation. The holding time for the sample heated at 1800°C was, therefore, limited to 10 min. To achieve faster secondary quenching rates than by air exposure, this sample was immersed in cold water.

Table 1 gives an overview of the different experiments. Fig. 2 shows a typical temperature versus time curve for a hybrid microwave heating/quenching experiment. The quenching possibility of the microwave furnace is a major advantage compared to most conventional furnaces were the total thermal mass is much higher and where opening of the furnace at elevated temperature and its exposure to air endangers the furnace components (e.g. thermocouples, heating elements, insulation...) due to the large thermal shock.

2.2. Materials

The investigated material was a top-grade rebonded magnesia-chromite refractory type (ANKROM S56, VRAG, Austria), manufactured from magnesia-chromite co-clinker. An increased density (3.38 g/cm^3) and low apparent porosity (12 vol.%) is achieved by means of salt impregnation. The resulting brick has a nominal composition (supplier data, in wt.%) of 60% MgO, 18.5% Cr_2O_3, 13.5% FeO_x, 6% Al_2O_3, 1.3% CaO and 0.5% SiO_2. Both virgin and industrially worn refractory

Table 1
Overview of the different hybrid microwave heating/quenching experiments

Refractory materials	Hold temperatures (°C)
As-delivered, virgin rebonded fused grain magnesia-chromite	1500–1600–1700
Industrially worn, slag infiltrated rebonded fused grain magnesia-chromite	1300–1400–1500–1550–1600–1650–1700–1750–1800[a]

[a] Held at 1800°C for 10 min before being quenched in water.

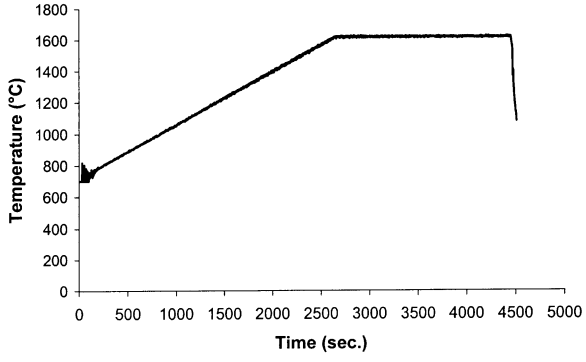

Fig. 2. Typical temperature versus time curve for a heating/quenching microwave experiment for a magnesia-chromite refractory specimen.

samples were used for the microwave experiments. The latter were obtained from a slag-line refractory brick, as recovered from a worn VOD ladle lining after 22 thermal cycles. From the remainder of the refractory brick, the top centimetre was removed with a diamond saw, as this part contained a slag layer which would become entirely liquid during the microwave experiments. The brick was divided into a number of smaller refractory specimens (e.g. 25 mm height, 25 mm^2 base) to fit in the conical alumina crucibles (Fig. 1). All quenched samples from the microwave experiments, cross-sections of the original industrially worn refractory brick, and specimens of the as-delivered magnesia-chromite material were prepared for microstructural analysis by means of SEM and EPMA. The samples were cut with a diamond saw, embedded in a resin (Technovit 4004) and ground with SiC grit. Carbon was evaporated on the sample surface to provide a conducting layer for microscopical analysis.

2.3. Experimental analysis techniques

The majority of the chemical analyses were performed by SEM/EPMA-EDS using a JEOL JXA-733 electron probe micro-analysis system equipped with an energy dispersive spectroscopy system from Tracor Northern (5400 Series), consisting of a beryllium window and a Si(Li) detector. The Semi-Quantitative (SQ) procedure from Tracor was used for quantitative elemental analysis. This program utilises the Phi-Rho-Z (PRZ) algorithm for quantitative correction of matrix effects in electron beam excited X-ray spectra. The SQ program requires that the operator selects a priori the oxides (e.g. FeO, Fe_2O_3, Cr_2O_3, Al_2O_3) or elemental compounds (e.g. Fe, Cr, Al) to be measured, as oxygen can not be determined directly with this EPMA-EDS setup. Although in the analysed refractory samples both FeO and Fe_2O_3 occur, for the sake of simplicity all FeO_x was determined as 'FeO'.

Elemental line scans, X-ray mappings and digital images for quantitative analyses were acquired with a high resolution SEM (Philips XL-30 FEG), equipped with an EDS detector system (from EDAX) with an ultra-thin window, enabling the qualitative determination of elements as light as boron. Line scans were generated using the eDXAUTO (Version 1.91, EDAX) software program. The mappings were obtained with the iDXi software (Version 2.3, EDAX), whereas the quantitative image processing/analysis was performed by assessing the digital images with the QWin software from LEICA.

3. Results and discussion

3.1. As-delivered rebonded magnesia-chromite

Fig. 3 shows backscattered electron (BSE) images of the investigated (as-delivered) rebonded magnesia-chromite refractory type. This material consists of periclase (magnesia), primary and secondary chromite (Mg,Fe)[Cr,Al,Fe]O_4 spinel and dicalciumsilicate ($2CaO.SiO_2$ or C_2S) phases. The latter cannot be seen on Fig. 3 since this phase is largely removed during sample preparation.[1–3] The chromite is present as large crystals (i.e. primary chromite) and as secondary chromite. Two types of secondary chromite can be distinguished. Type I is formed by intergranular precipitation during cooling and is located at periclase grain boundaries, exsolved out of periclase (Ia) or crystallised from spinel-rich liquid (Ib). Type II arises from intragranular exsolution precipitation from periclase grains on cooling, and thus forms within these periclase grains.[1,13] The as-delivered microstructure of this refractory type is characterised by a high proportion of direct bonding between the periclase matrix and the chromite, i.e. a direct attachment without any intermediate silicate film.[13] Direct bonded (and rebonded) magnesia-chromite refractories display enhanced mechanical and refractory properties (e.g. hot

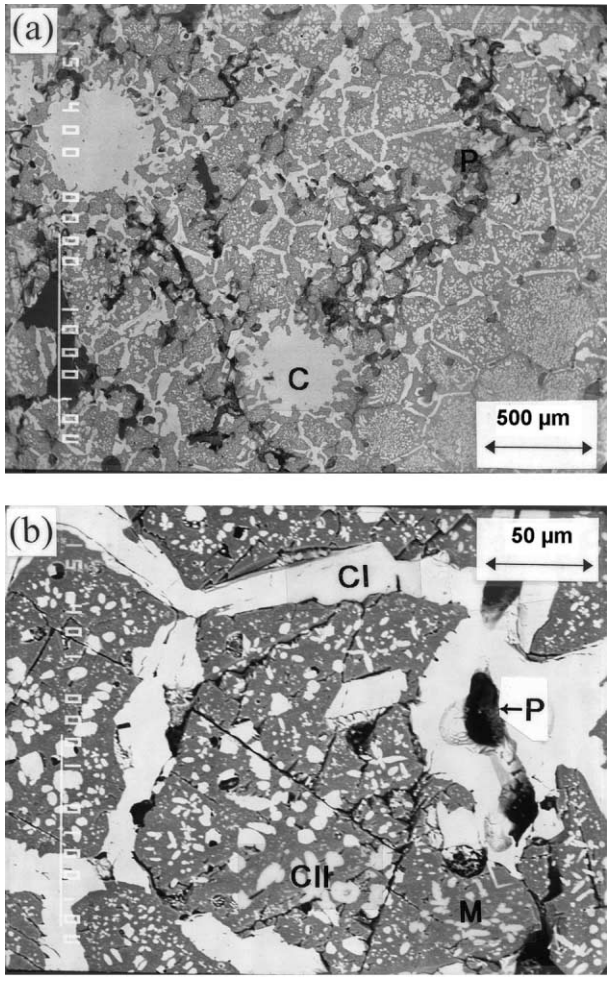

Fig. 3. BSE micrographs of as-delivered rebonded magnesia-chromite refractory brick: Per = magnesia (periclase); C = primary chromite; CI = secondary chromite type I, CII = secondary chromite type II; P = pore.

temperature strength, slag resistance, dimensional stability) compared to their chemically bonded counterparts. The intergranular secondary chromite (type Ia and Ib) is not only of great significance for the direct bonding but also for the protection against slag penetration. Top-grade rebonded magnesia-chromite refractories should therefore be designed in such a way that the periclase grain boundaries are secured against slag infiltration. This is achieved by an optimum choice of raw materials (ratio, size distribution, composition) and firing parameters in order to allow a uniform crystallisation and distribution of (intergranular) secondary chromite throughout the matrix, during the slow cooling after the firing process.[14]

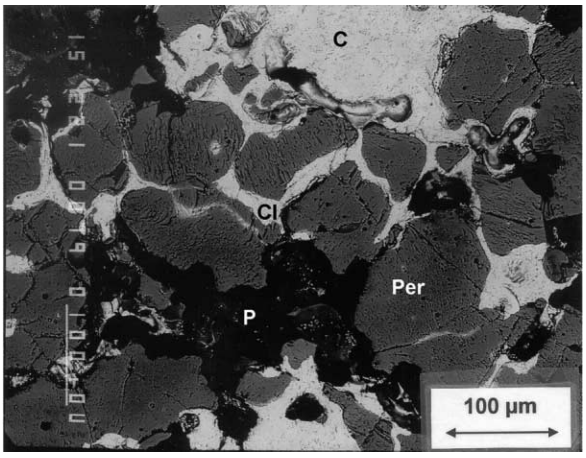

Fig. 4. BSE micrograph of as-delivered rebonded magnesia-chromite refractory brick, reheated/quenched from 1700°C: Per = magnesia (periclase); C = primary chromite; CI = secondary chromite type I; P = pore.

3.2. As-delivered reheated/quenched magnesia-chromite

Fig. 4 presents BSE images of the as-delivered specimen quenched from 1700°C, clearly illustrating that the remaining amount of non-dissolved secondary chromite was fairly limited, compared with the slowly cooled material (Fig. 3). Table 2 shows the EPMA results for the chromite and periclase phases, as a function of temperature. Global analyses are also presented. The reported values are the means and standard deviations of at least six measurements at different positions in the same sample. From Table 2, the following conclusions can be drawn:

1. The difference in FeO_x content in the primary (11 wt.%) and secondary chromite (20 wt.%) in the as-delivered material is the result of the different affinity of magnesia (MgO) for (in decreasing order) FeO_x, Cr_2O_3 and Al_2O_3. During refractory production, surplus MgO diffuses into the chromite forming MgO-rich spinel, while FeO_x and, to a lesser extent, Cr_2O_3 and Al_2O_3 are able to diffuse into the periclase forming a solid solution. During cooling after the firing process, FeO_x-rich secondary spinel (type Ia, Ib and II) is precipitated/exsolved out of the periclase solid solution, leaving almost pure magnesia (i.e. 95 wt.% MgO, Table 2) in its wake.

Table 2
Chemical composition of the various refractory phases in the as-delivered rebonded magnesia-chromite refractory brick as a function of temperature, as obtained by EPMA

Refractory phase	Temperature (°C)	MgO (wt.%)	CaO (wt.%)	SiO_2 (wt.%)	Al_2O_3 (wt.%)	Cr_2O_3 (wt.%)	FeO[c] (wt.%)
Periclase	as-del[a]	95±1	<0.5	<0.5	<1	1.9±1.1	1.7±1.2
	1500	77.2±0.7	<1	<0.5	2.3±0.3	8.8±0.5	10.4±0.3
	1600	69±3	<1	<0.5	3.5±0.6	13±1	13±1
	1700	68±2	<1	<0.5	3.8±0.6	14±1	14±1
Secondary chromite Ia	as-del	21±2	0.5±0.1	<0.5	15.1±0.2	42±1	20±2
	1500	20.4±0.3	0.6±0.1	<0.5	15.5±0.5	43±1	19±1
	1600	21±2	0.6±0.3	<0.5	15.1±0.6	44±1	19±1
	1700	22±2	0.6±0.2	<0.5	15.8±0.3	46±1	14.6±0.2
Primary chromite	as-del	18.3±0.6	1.0±0.7	<1	15.9±0.3	52±2	11±1
	1500	18±1	0.5±0.1	<0.5	14.5±0.8	53±1	14±2
	1600	18.6±0.5	0.4±0.1	<0.5	15.7±0.7	53±1	12±1
	1700	17±1	0.8±0.2	<0.5	15.0±0.6	53±1	13±1
Global analysis	as-del	59±4	–[b]	–	6.2±0.8	20±2	11.9±0.4
	1500	58±2	–	–	6.7±0.8	21±2	13.4±0.6
	1600	56±3	–	–	7±1	22±2	14.1±0.8
	1700	58±2	–	–	6.6±0.5	21±2	13.5±0.3

[a] as-delivered.
[b] Not determined due to Ca and Si contamination during sample preparation (calciferous rinsing water and Technovit resin infiltrate the cracks generated during quenching).
[c] All iron oxide inside the brick was expressed as 'FeO' for the sake of simplicity.

2. With increasing temperature (similar as during the firing process), FeO_x and Cr_2O_3, mainly from the secondary spinel phases dissolve into the periclase phase (13 wt.% FeO_x and 14 wt.% Cr_2O_3 at 1700°C). The concentration of Al_2O_3 in periclase is less extensive (i.e. 3.8 wt.% at 1700°C), but higher than expected from the the binary system MgO–Al_2O_3 (i.e. 2 wt.% at 1680°C). This is in agreement with the findings of Dewendra et al.,[6,9–11] who concluded that the solid solubility of Al_2O_3 and Cr_2O_3 in periclase is influenced by the presence of other oxides. Thus, the Al_2O_3 solubility increases in the presence of both FeO_x and Cr_2O_3.
3. The composition of the primary chromite crystals is fairly independent of the temperature. The primary chromite grains play a minor role in the protection against slag penetration.
4. The concentration of CaO and SiO_2 in the periclase and spinel phases is limited, in accordance with the work of Dewendra et al.[10]

From the above, it can be concluded that the as-delivered rebonded magnesia-chromite refractory intrinsically suffers from high-temperature inactivation of the protective and direct bonding secondary chromite phases through dissolution into the enveloping periclase phase. At temperatures in excess of 1700°C, the rebonded magnesia-chromite brick is gradually depleted from its intergranular secondary chromite phase, in effect transforming into a magnesia brick. This results in an increased susceptibility to slag infiltration. It is generally accepted that the intrinsic weakness of magnesia relative to magnesia-chromite bricks is due to the fact that the ability of a liquid to penetrate between periclase grains is considerably higher than between periclase/spinel grains, because of the requirement for the system to minimise its total surface energy.[14,15] Any liquid formed in the interior of the brick at elevated temperatures or infiltrated during the VOD process would swiftly seep through the weakened brick structure.

3.3. Industrially worn in situ (slowly) cooled magnesia-chromite

Figs. 5 and 6 are BSE images of the investigated industrially worn refractory sample as recovered from the VOD ladle after slow in situ cooling. Fig. 5a is a cross-section of the hot face of the worn brick. The typical features, as described previously,[1] can be recognised: FeO_x-decomposition and the formation of iron-rich metallic particles, primary chromite degradation (Fig. 5B), dissolution of secondary chromite type II into the periclase and severe slag infiltration.

Fig. 6 is a BSE micrograph taken at 15 mm distance from the hot face. The compositions of the different phases present in this zone were determined with

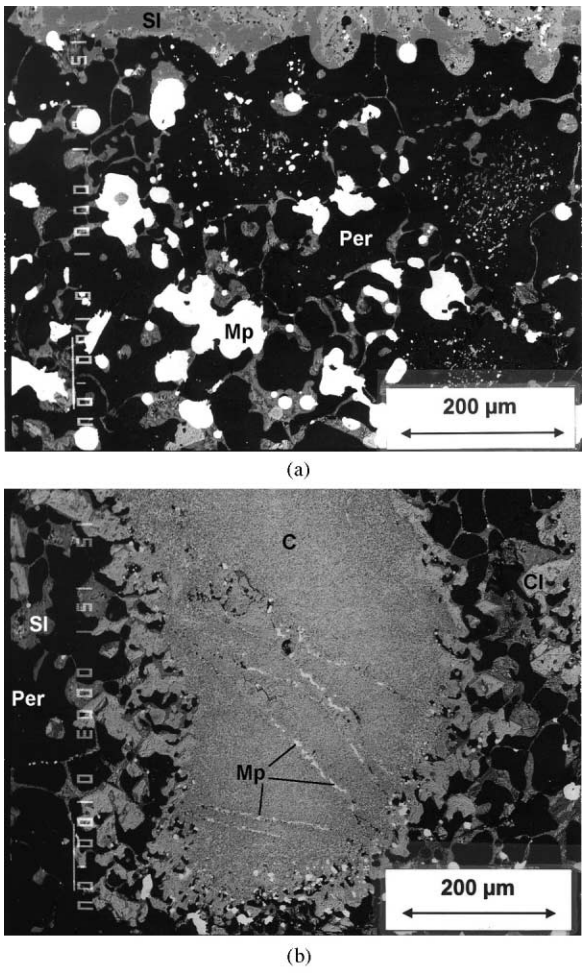

Fig. 5. BSE micrographs of the hot face of industrially worn rebonded magnesia-chromite refractory brick as recovered from the VOD ladle lining, showing a cross-section (a) and a degraded primary chromite crystal (b): Per = magnesia(periclase); C = primary chromite; CI = secondary chromite type I; Mp = metallic(iron-rich) particle; SI = slag.

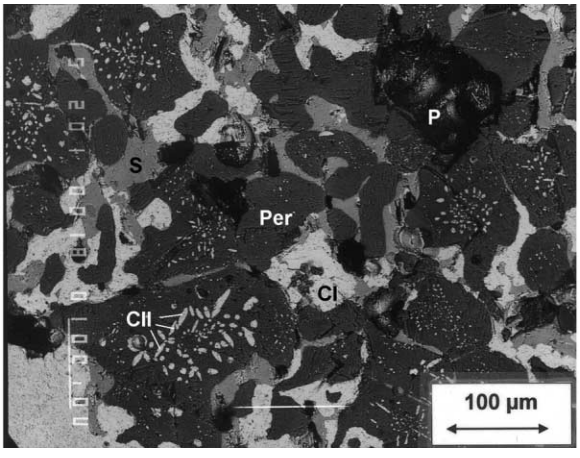

Fig. 6. BSE micrograph at 15 mm from the hot face of industrially worn debonded magnesia-chromite refractory brick as recovered from the VOD ladle lining: Per = magnesia(periclase); CI = secondary chromite type I, CII = secondary chromite type II; P = pore or crack, S = merwinite.

EPMA-EDS (Table 3). The results for the primary chromite are omitted as they are not relevant for this investigation. The large standard deviations (based on six measurements) for the global composition of the analysed specimen are due to the heterogeneity of the material.

Fig. 6 demonstrates why post-mortem analysis of industrial samples can sometimes lead to ambiguous insights. This is especially the case for the assessment of the actual state of the secondary chromite (type I) phase during industrial exposure. Fig. 6 suggests that this phase was solid at the operating temperature as it coexists with merwinite ($3CaO.MgO.2SiO_2$ or C_3MS_2). However, the refractory structure seen in Fig. 6 is not the actual state of the magnesia-chromite brick at the elevated VOD temperature due to the relatively slow cooling rate of the ladle, as is shown in the next sections. A similar, although less severe, evaluation difficulty arises for the secondary chromite (type II) phase.

3.4. Industrially worn reheated/quenched magnesia-chromite

3.4.1. Destruction of the microstructure during heating

Fig. 7a is a SEM image of the industrially worn sample quenched from 1300°C, which demonstrates that the refractory microstructure was entirely solid at this temperature. The merwinite phase coexists with the secondary chromite type I whereas the presence of a considerable amount of secondary chromite type II inside the periclase grains is clearly visible.

At 1400°C (Fig. 7b) the merwinite partially reacted with the secondary chromite type I and formed a small quantity of liquid phase. At 1500 and 1600°C, the melt formation was more pronounced. Fig. 8 shows a grey area inside the specimen quenched from 1600°C, which is the minimum temperature encountered in the VOD process. We believe that this phase is quenched liquid due to its uniform (periclase) enveloping structure and the occurrence of small precipitates (some of them growing from the periclase grain boundary). These bright crystals were clearly formed during (imperfect) primary quenching. EPMA-EDS analysis showed that they are a chromium-free spinel phase (i.e. (Mg,Fe)[Al,Fe]O_4). Fig. 8 also shows that the secondary chromite type II largely dissolved into the periclase.

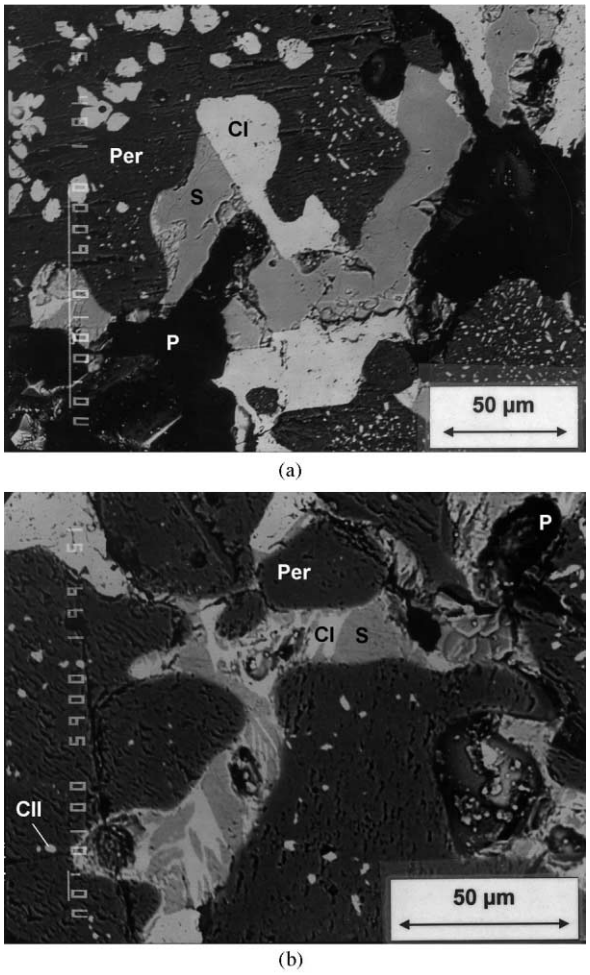

Fig. 7. BSE micrographs of industrially worn rebonded magnesia-chromite refractory brick reheated/quenched from 1300°C (a) and 1400°C (b): Per = magnesia(periclase) phase; CI = secondary chromite type I, CII = secondary chromite type II; P = pore or crack, S = merwinite.

At 1700°C (Fig. 9a), which can be considered as the average temperature during the VOD process, the remaining amount of secondary chromite type II was rather limited, whereas melting had continued rapidly. The amount of protective secondary chromite type I was strongly depleted, resulting in substantial liquid penetration along the periclase grain boundaries. Fig. 9b shows the liquid fraction at higher magnification. Similar to Fig. 8, a minor precipitation of chromium-free

Table 3
Global analysis and composition of the periclase and chromite refractory phases of 15 mm from the hot face in an industrially worn rebonded magnesia-chromite refractory brick, as obtained by EPMA

Refractory phase	MgO (wt.%)	CaO (wt.%)	SiO_2 (wt.%)	Al_2O_3 (wt.%)	Cr_2O_3 (wt.%)	FeO (wt.%)
Periclase	77±1	<0.5	<0.5	1.8±0.3	8.0±0.5	11.4±0.8
Secondary chromite I	20±1	0.5±0.1	<0.5	14±2	40±1	24±1
Secondary chromite II	20±1	0.5±0.1	<0.5	13.8±0.3	41±1	22.8±0.4
Global analysis	49±2	8±1	4.1±0.5	7±1	20±2	12.4±0.8

spinel occurred during primary quenching. At 1750°C, similar remarks as for Fig. 9a are valid but the observed phenomena were far more pronounced.

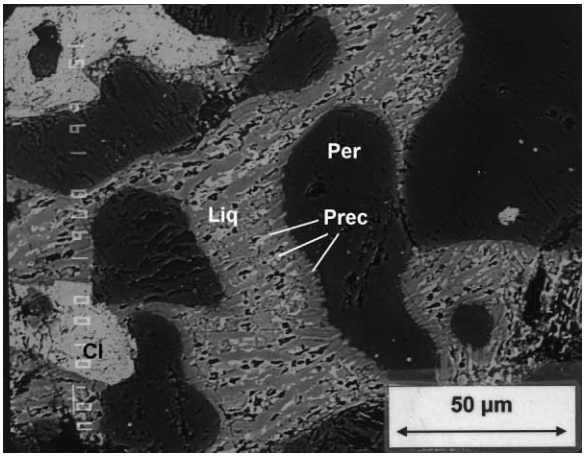

Fig. 8. BSE micrograph of industrially worn rebonded magnesia-chromite refractory brick reheated/quenched from 1600°C: Per = magnesia (periclase); CI = secondary chromite type I; Liq = liquid slag phase; Prec = $MgO.(Al,Fe)_2O_3$ spinel precipitates.

From 1750°C onwards any temperature increase is catastrophic, as can be seen from Fig. 9c and d (1800°C). Primary chromite grains were heavily attacked and infiltrated, secondary chromite phases (both type I and II) were absent, whereas an infiltrated network of liquid silicate slag annihilated the entire brick structure. The slag phase almost completely wetted the periclase grains. The resulting dihedral angle $\phi_{per\text{-}per}$ (i.e. the angle formed in the neck between neighbouring periclase grains by the liquid phase) was close to zero. This confirms the findings of both Hayhurst and Laming[7] as White,[14] who observed that, for a given composition of a magnesia-chromite mixture, $\phi_{per\text{-}per}$ decreased considerably with increasing temperature. Fig. 9d shows in detail the liquid slag phase quenched from 1800°C. In this case, no spinel precipitation occurred during quenching. This is probably due to the larger driving force for primary quenching.

The homogeneity of the quenched (amorphous) liquid phase allowed an accurate quantitative image analysis to calculate the volume fraction of the slag phase. However, due to the intrinsic heterogeneity of the magnesia-

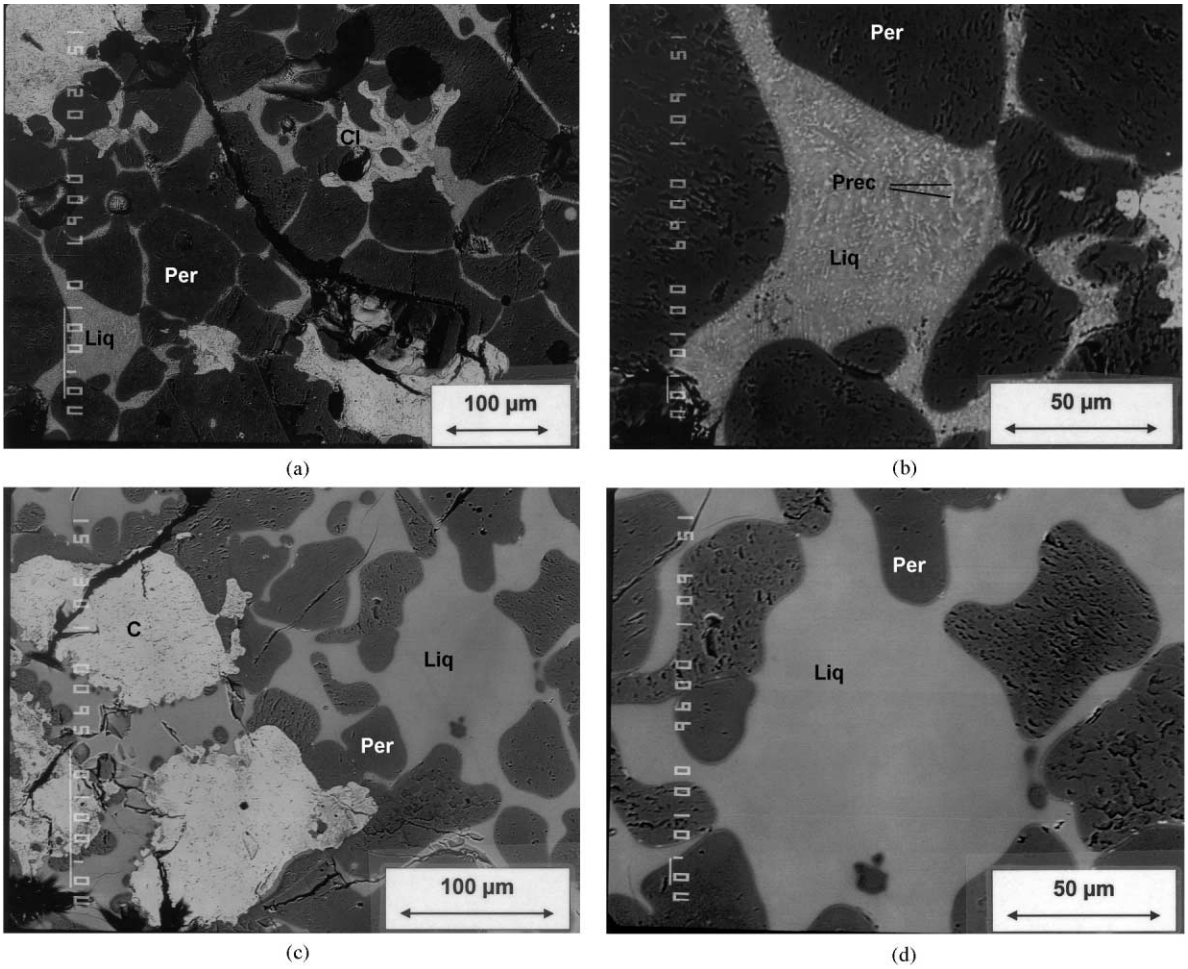

Fig. 9. BSE micrographs of industrially worn rebonded magnesia-chromite refractory brick reheated/quenched from 1700°C (a,b) and 1800°C (c,d): Per = magnesia (periclase); CI = secondary chromite type I; Liq = liquid slag phase; Prec = $MgO.(Al,Fe)_2O_3$ spinel precipitates.

chromite refractory sample itself, a high number of images had to be processed to obtain a reliable average value. A program was written with the QWin software to automate the assessment of the SEM images. Furthermore, this procedure had to correct for the large number of cracks which arose during rapid quenching. Fig. 10 shows the liquid (10b) and crack fraction (10c) for a typical image of the refractory specimen quenched from 1800°C (10a). With this method, based on 24 images at a magnification of 65, an average value of 13±3 vol.% liquid was estimated.

Such a high liquid fraction indicates that at 1800°C the refractory had become almost entirely liquid-bonded and would therefore be extremely susceptible to detrimental erosion and spalling mechanisms.

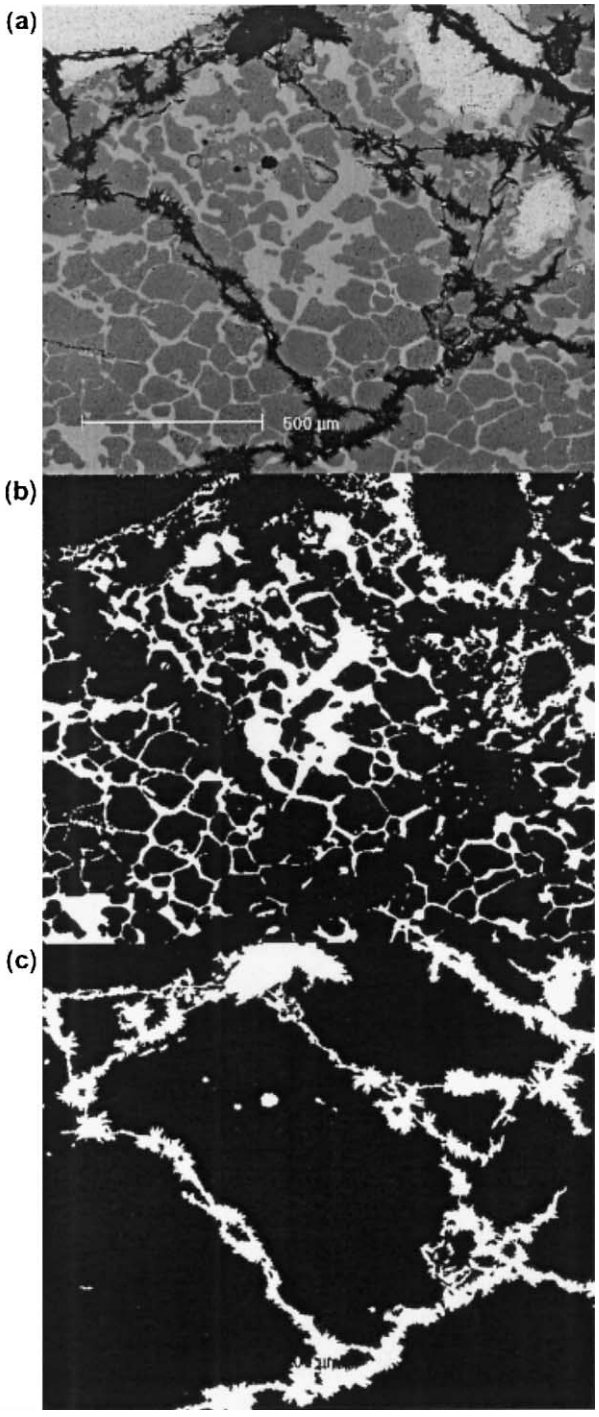

Fig. 10. SEM micrograph (a) of an industrially worn rebonded magnesia-chromite refractory brick reheated/quenched from 1800°C, and quantative image processing/analysis highlighting the quenched liquid (b) and the crack (c) fraction.

3.4.2. Liquid phase composition as a function of temperature

The infiltrating VOD slag phase typically contains 35–45 wt.% CaO, 30–40 wt.% SiO_2, 5–8 wt.% MgO, 2–5 wt.% Al_2O_3 and some minor components such as CaF_2, MnO, FeO and Cr_2O_3. This VOD slag however is clearly different from the quenched liquid slag phases inside the brick. Fig. 11a and Table 4 show the composition of this liquid phase as a function of temperature. The results were obtained from at least six global analyses of the liquid zones. The relatively large standard deviations, for the temperature range 1500–1750°C, are the result of the heterogeneity of the imperfectly quenched liquid phase. At all temperatures, the dissolved Cr_2O_3 content was very low (< 1 wt.%), whereas Al_2O_3 (> 6 wt.%) and FeO_x (> 7 wt.%) easily dissolved into the liquid silicate phase. MgO also dissolved into the slag phase, reaching a maximum content of 15 wt.% at 1800°C. This is in agreement with previous findings on MgO saturation in stainless steel

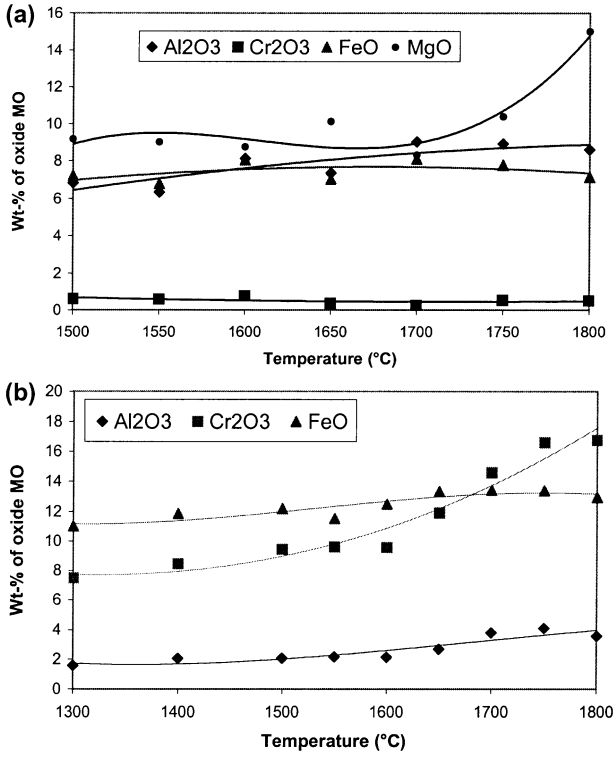

Fig. 11. Liquid phase (a) and periclase (b) composition in quenched industrially worn rebonded magnesia-chromite refractory brick, as a function of temperature.

Table 4
Liquid phase composition in quenched industrially worn rebonded magnesia-chromite refractory brick, as a function of temperature, as obtained by EPMA

Temperature (°C)	MgO (wt.%)	CaO (wt.%)	SiO_2 (wt.%)	Al_2O_3 (wt.%)	Cr_2O_3 (wt.%)	FeO (wt.%)
1500	9±1	48±3	25±2	7±2	0.6±0.2	7±2
1550	9±1	46±1	29±1	6.3±0.4	0.6±0.2	7±1
1600	9±1	47±2	25±1	8.1±0.4	0.8±0.3	8±1
1650	10±2	43±2	31±2	7±1	0.4±0.2	7±1
1700	8±1	44±2	28±1	9±1	0.3±0.1	8±1
1750	11±2	39±1	32±1	9±1	0.5±0.2	7±1
1800	15.0±0.8	35±1	32±1	8.6±0.7	0.5±0.2	7.1±0.7

slags.[1–5] From the experimental data it can be concluded that, although the infiltrated slag dissolved MgO, FeO_x and Al_2O_3 from both the periclase as the chromite spinel phases, it did not significantly attack the Cr_2O_3 component in those phases. This is a refinement of the observations of Hayhurst and Laming[7] who indicated that a considerable amount of Al_2O_3, iron oxide and, possibly, Cr_2O_3 dissolves into the liquid phase of a chrome-magnesite refractory at high temperature.

The extra low values of dissolved Cr_2O_3 found in this work can be qualitatively explained by comparing them with the saturation concentration of Cr_2O_3 in stainless steel slags at VOD processing temperatures. According to Turkdogan,[16] this saturation value is about 5 wt.%, at which the activity of Cr_2O_3 becomes unity. In the magnesia-chromite brick at 1800°C, apart from some primary chromite crystals, the only remaining phases are periclase (containing 17 wt.% Cr_2O_3, 12.9 wt.% FeO_x, and 3.6 wt.% Al_2O_3, see Table 5) and spinel-rich liquid slag (with a Cr_2O_3 content of 0.5 wt.%). Assuming equilibrium between these two phases, the low dissolved Cr_2O_3 content is plausible as the Cr_2O_3 activity in the periclase (with a molar fraction of 6%) is considerably less than unity.

3.4.3. Periclase phase composition as a function of temperature

Table 5 and Fig. 11b show the periclase phase composition as a function of the temperature. These values are quite similar to those of the as-delivered magnesia-chromite (Table 2). The relatively large standard deviations are due to the heterogeneity of the material. In a chromite-rich zone, the periclase contains a higher amount of FeO_x, Cr_2O_3 and Al_2O_3 than in a magnesia-rich area. In general though, the presencce of FeO_x and Cr_2O_3 in the periclase solid solution increased considerably at higher temperatures. On the other hand, Al_2O_3 dissolved/diffused into periclase in a limited way, as it clearly preferred the liquid slag phase.

3.4.4. Distribution of elements at 1800°C

The findings reported in the two previous sections were qualitatively confirmed by line scan analyses (Fig. 12) and X-ray mapping experiments (Fig. 13) on the industrially worn sample quenched from 1800°C. The line scan passes through a liquid zone, a periclase grain and the remainings of a primary chromite crystal, containing a little liquid droplet in the middle of the grain (Fig. 12a). The mapping was obtained from a region that consisted of a liquid phase network, periclase grains and a degraded primary chromite particle (Fig. 13a). From these data, a number of observations and confirmations concerning the distribution of the various refractory elements/components at high temperatures can be made:

1. Cr_2O_3 does not dissolve into the liquid phase, as is proven by the sharp decrease in chromium in the small liquid area inside the primary chromite

Table 5
Periclase composition in quenched industrially worn rebonded magnesia-chromite refractory brick, as a function of temperature, as obtained by EPMA

Temperature (°C)	MgO (wt.%)	CaO (wt.%)	SiO_2 (wt.%)	Al_2O_3 (wt.%)	Cr_2O_3 (wt.%)	FeO (wt.%)
as-recovered	77±1	<0.5	<0.5	1.8±0.3	8.0±0.5	11.4±0.8
1300	79±2	<0.5	<0.5	1.6±1.2	7.5±0.8	11±1
1400	76.3±0.4	<0.5	<0.5	2.0±0.1	8.5±0.4	11.8±0.3
1500	75.3±0.5	<0.5	<0.5	2.1±0.3	9.4±0.3	12.2±0.4
1550	76±1	<0.5	<0.5	2.2±0.3	9.6±0.7	11.5±0.3
1600	75±2	<0.5	<0.5	2.1±0.3	9.6±0.6	12±2
1650	71±2	<0.5	<0.5	2.7±0.4	12±1	13±1
1700	67±1	<0.5	<0.5	3.8±0.3	14.6±0.9	13.4±0.6
1750	64±2	<0.5	<0.5	4.1±0.7	16.6±0.9	13.4±0.9
1800	66±2	<0.5	<0.5	3.6±0.9	17±2	12.9±0.6

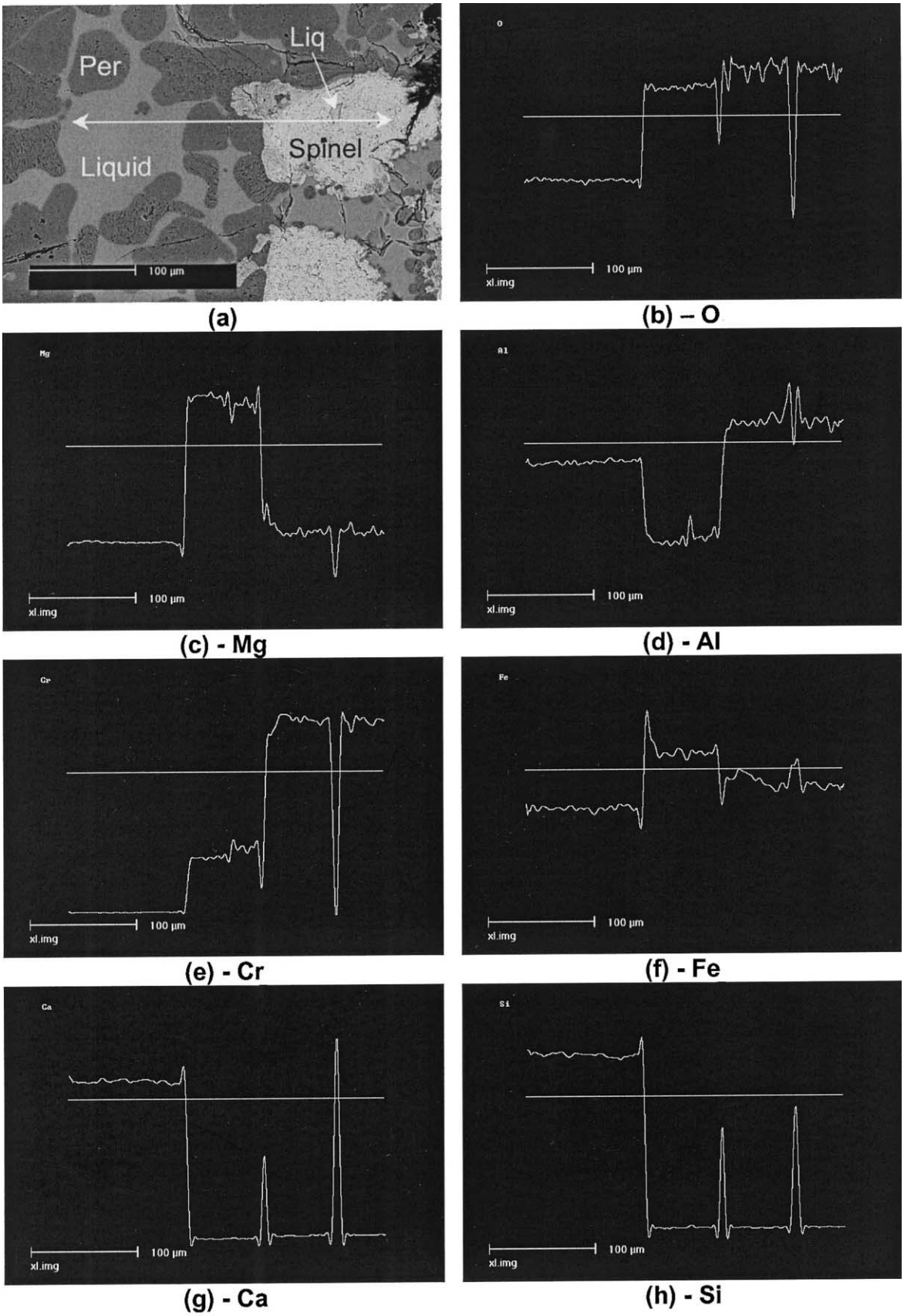

Fig. 12. Line scans (O, Mg, Al, Cr, Fe, Ca and Si) (b through h) for industrially worn rebonded magnesia-chromite refractory, quenched from 1800°C, for a SEM image (a) (256 pixels* 16394 ms dwell time).

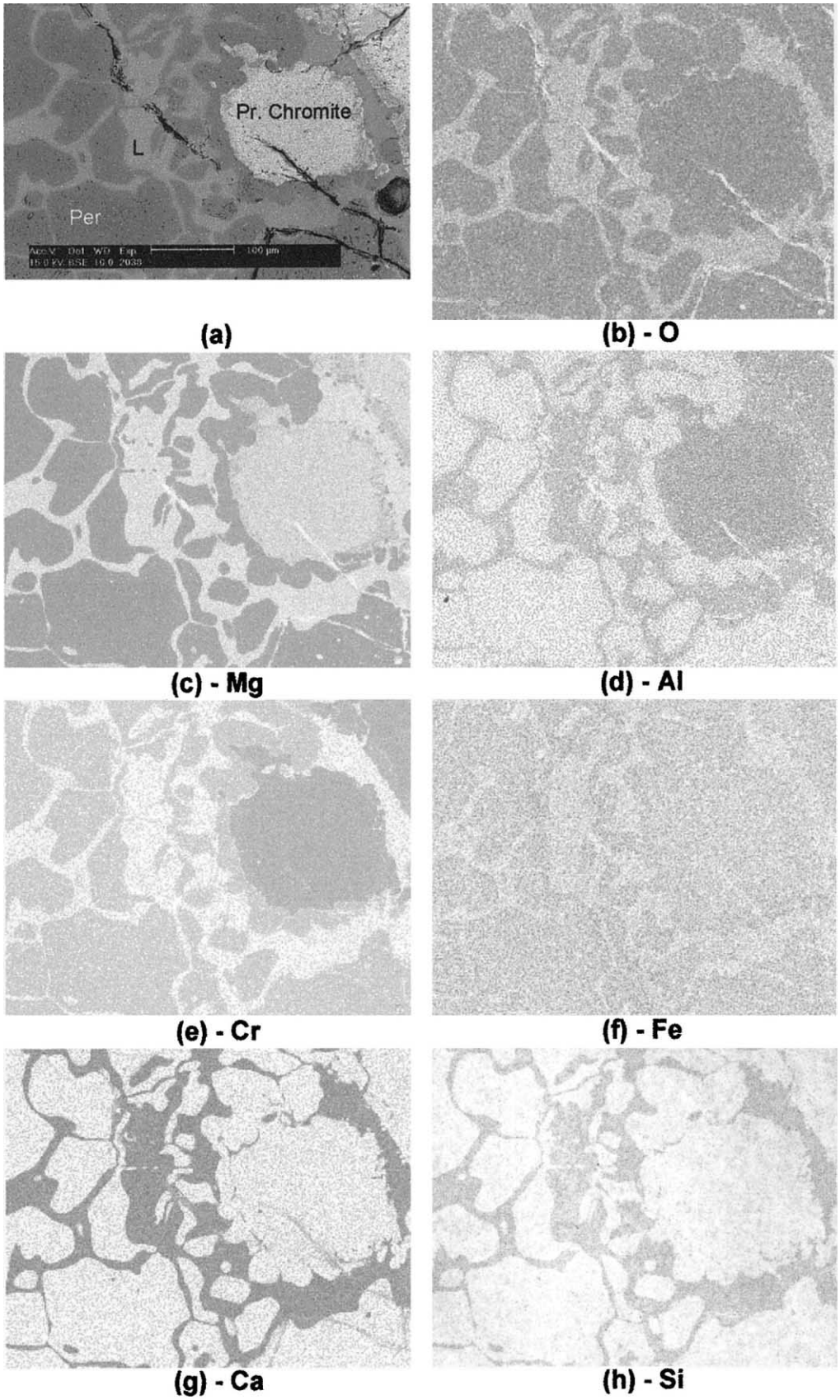

Fig. 13. X-ray mapping data (O, Mg, Al, Cr, Fe, Ca and Si) (b through h) of industrially worn rebonded magnesia-chromite refractory, quenched from 1800°C, for a SEM image (a).

particle (Fig. 12e). Cr_2O_3 from the secondary chromite spinel almost completely dissolves into the periclase phase.
2. FeO_x is evenly distributed among the periclase and the liquid slag phase (Fig. 12f and 13f).
3. MgO and Al_2O_3 substantially dissolve into the liquid phase (Figs. 13c and 12d), whereas the Al_2O_3 solubility in the periclase phase is fairly limited (Fig. 13d).
4. Figs. 13g and 13h are almost exact replicas of each other, as CaO and SiO_2 form the basis of the slag phase and neither dissolve in the solid phases.

3.4.5. Refractoriness of spinel components

Some important conclusions can be drawn on the refractoriness of complex $(Mg,Fe)[Cr,Al,Fe]O_4$ spinel, which is a solid solution of $MgO.Cr_2O_3$ (magnesiochromite, MK), $MgO.Al_2O_3$ (spinel, MA) and $MgO.Fe_2O_3$ (magnesioferrite, MF) spinel. It has been shown that the protective and direct bonding secondary chromite phase can be inactivated at elevated temperatures by two mechanisms: (1) dissolution into the periclase phase, and (2) dissolution in the liquid slag phase. The latter mechanism is considered to be predominant. MK is exclusively subjected to mechanism (1), whereas MA is only significantly susceptible to mechanism (2). MF spinel however, is subjected to both (1) and (2). Regarding the influence of the composition of the periclase solid solution, iron oxide (and Al_2O_3) decreases the dihedral angle $\phi_{per\text{-}per}$ for the periclase-liquid slag system, whereas Cr_2O_3 increases $\phi_{per\text{-}per}$.[14] At high temperatures, where both Cr_2O_3 and FeO_x are largely dissolved into the periclase, the magnesia-MK system is assumed to be far more resistant to slag ingress than the magnesia-MF system, due to its higher dihedral angle. The different contributors to the spinel phase in a magnesia-chromite brick can be classified according to their refractoriness as: MK > MA≫MF. The refractoriness of MF spinel in VOD ladle linings is further diminished due to its susceptibility to decomposition as a result of low oxygen partial pressures (10^{-9}–10^{-4} Pa).[1] From this, it can be concluded that the presence of FeO_x in the raw materials for commercial magnesia-chromite production is completely undesirable.

4. Conclusions

The high-temperature inactivation of the secondary chromite phase in both as-delivered and industrially worn rebonded magnesia-chromite refractories was investigated using a cylindrical single-mode hybrid microwave heating furnace. Samples were slowly heated, held at a specified elevated temperature, quenched and further analysed with SEM, EPMA-EDS and quantitative image analysis. The experimental setup allowed to achieve a maximum temperature of 1800°C which is 100°C higher than in existing studies[6,7] on magnesia-chromite behaviour at high temperatures. These temperatures in excess of 1700°C were of primary importance to simulate actual industrial VOD conditions.

This work resulted in the quantification of the high-temperature inactivation of the secondary chromite phases, refining the experimental observations of previous work. Two parallel inactivation mechanisms occur: dissolution (1) in the periclase phase and (2) in the liquid slag. As-delivered magnesia-chromite refractories are exclusively exposed to mechanism (1). The inactivation of secondary chromite is far more precarious in slag-infiltrated bricks which suffer from (1) and (2), with (2) being predominant.

Some important conclusions can now be drawn. With respect to resistance to the high-temperature inactivation, a synthetic magnesia-MK spinel refractory would be superior to commercial magnesia-chromite as well as synthetic magnesia-MA spinel bricks. However, a magnesia-MK brick would be extremely expensive to manufacture and, furthermore, undesirable for environmental reasons.[17,18] A workable and realistic alternative for the investigated top-grade magnesia-chromite brick in the slag line of VOD ladle linings is not straightforward, due to the extremely harsh conditions imposed on the lining.

Concurrently, this work demonstrates that hybrid microwave heating is a powerful alternative for conventional furnace experiments on refractory samples, due to its quenching capabilities, user-friendliness, inexpensiveness and reproducibility. Future work will include the further optimisation of the quenching velocity by exposing the samples to a controlled stream of liquid nitrogen.

Acknowledgements

The authors are grateful for financial support from ALZ (Genk, Belgium). Prof W.E. Lee from the University of Sheffield is acknowledged for his useful comments and ideas about refractory wear investigation. We are also extremely thankful to Rudy De Vos for his professional assistance with the Philips XL-30 measurements and the quantitative image analyses.

References

1. Jones, P. T., Blanpain, B., Wollants, P., Ding, R. and Hallemans, B., Degradation mechanisms of magnesia-chromite refractories in vacuum-oxygen decarburisation ladles during the production of stainless steel. *Ironmaking and Steelmaking*, 2000, **27**(3), 228–237.
2. Jones, P.T., Blanpain, B., Wollants, P., Ding, R., Hallemans, B., Heylen, G. and Weytjens, J., Degradation mechanisms of magnesia-chromite refractories in VOD ladles and measures to extend the lining life. In *Proceedings of the 6th Conference on Molten Slags, Fluxes and Salts*. Stockholm/Helsinki, 2000, www.slags2000.kth.se (po335.pdf).

3. Jones, P. T., Blanpain, B., Wollants, P., Hallemans, B., Heylen, G. and Weytjens, J., Extending the lining life of ALZ nv's ladle lining. *Iron and Steelmaker*, 1999, **26**(12), 31–35.
4. Jones, P. T., Blanpain, B., Wollants, P. and Hallemans, B., Chemical interactions of magnesia-chromite refractories with liquid phases during the secondary refinement of stainless steel. In *Proceedings of the 5th International conference on progress in analytical chemistry in the steel and metals industries*, ed. R. Tomellini. European Communities, Belgium, 1999, pp. 602–609.
5. Blanpain, B., Jones, P.T., Vichev, R.G. and Wollants, P., Chemical micro-analysis of metallurgically worn magnesia-chromite refractory materials. In *Proceedings of the 7th European Conference on Applications of Surface and Interfacial Analysis,* ed. I. Olefjord et al. Chichester, 1997, pp. 239–242.
6. Dewendra, J. D., Wilson, C. M. and Brett, N. H., A quantitative investigation of phase compositions in magnesia-R_2O_3-silicate systems, Part 4. *Trans. J. Br. Ceram. Soc*., 1983, **82**, 132–136.
7. Hayhurst, A. and Laming, J., The structure of chrome-magnesite refractories at high temperatures. *Trans. J. Br. Ceram. Soc*., 1963, **62**, 989–1005.
8. Serry, M. A., Othman, A. G. M., Girgis, L. G. and Weisweiler, W., Phase equilibrium, microstructure and properties of some magnesite-chromite refractories. *J. Mat. Science*, 1996, **31**, 4913–4920.
9. Dewendra, J. D., Wilson, C. M. and Brett, N. H., A quantitative investigation of phase compositions in magnesia-R_2O_3-silicate systems, Part 1. *Trans. J. Br. Ceram. Soc*., 1982, **81**, 185–189.
10. Dewendra, J. D., Wilson, C. M. and Brett, N. H., A quantitative investigation of phase compositions in magnesia-R_2O_3-silicate systems, Part 2. *Trans. J. Br. Ceram. Soc*., 1983, **82**, 64–68.
11. Dewendra, J. D., Wilson, C. M. and Brett, N. H., A quantitative investigation of phase compositions in magnesia-R_2O_3-silicate systems, Part 3. *Trans. J. Br. Ceram. Soc*., 1983, **82**, 87–90.
12. Zhao, C., Vleugels, J., Groffils, C., Luypaert, P. J. and Van der Biest, O., Hybrid sintering with a tubular susceptor in a cylindrical single-mode microwave furnace. *Acta Mater*., 2000, **48**, 3795–3801.
13. Goto, K., Argent, B. B. and Lee, W. E., Corrosion of MgO-$MgAl_2O_4$ spinel refractory bricks by calcium aluminosilicate slag. *J. Am. Ceram. Soc*., 1997, **80**(2), 461–471.
14. White, J. and Richmond, C., Recent developments in research on basic refractories — 2. *Refractories J*., 1970, **46**, 6–18.
15. Stephenson, I. M. and White, J., Factors controlling microstructure and grain growth in two-phase (one solid + one liquid) and in three-phase (two solid + one liquid) systems. *Trans. J. Br. Ceram. Soc*., 1966, **65**, 443–483.
16. Turkdogan, E. T., *Physicochemical Properties of Molten Slags and Glasses*. The Metals Society, London, UK, 1983.
17. Lee, Y. and Nassaralla, C. L., Minimization of hexavalent chromium in magnesite-chrome refractory. *Met. Trans*., 1997, **28B**, 855–859.
18. Lee, Y. and Nassaralla, C. L., Formation of hexavalent chromium by reaction between slag and magnesite-chrome refractory. *Met. Trans*., 1998, **29B**, 405–410.